

ARTICLE OPEN



Implication of human endogenous retrovirus W family envelope in hepatocellular carcinoma promotes MEK/ERK-mediated metastatic invasiveness and doxorubicin resistance

Yan Zhou^{1,5}, Lijuan Liu^{1,5}, Youyi Liu^{1,2}, Ping Zhou¹, Qiuji Yan¹, Honglian Yu^{1,3}, Xiaobei Chen⁴ and Fan Zhu¹✉

© The Author(s) 2021, corrected publication 2022

Human endogenous retrovirus (HERVs), originating from exogenous retroviral infections of germ cells millions of years ago, have the potential for human diseases. Syncytin-1, an envelope protein encoded by the HERV W family, participates in the contexts of schizophrenia, multiple sclerosis, diabetes, and several types of cancers. Nevertheless, there is no report on the expression pattern and potential mechanism of Syncytin-1 in HCC. Here we found Syncytin-1 expression was up-regulated in HCC compared to adjacent non-tumorous tissues, especially in advanced HCC. Syncytin-1 was an independent risk factor to predict vascular invasion, metastasis, larger tumor size, and poor prognosis in HCC patients. Further analysis discovered that Syncytin-1 overexpression positively associated with HCC patients with serum HBsAg positive. Functional experiments in vitro and in vivo demonstrated that Syncytin-1 enhanced cell proliferation, metastasis, and tumorigenicity in HCC. Kyoto Encyclopedia of Genes and Genomes (KEGG) pathway analysis suggested that the mitogen-activated protein kinase (MEK)/extracellular signal-regulated protein kinase (ERK) pathway was involved in HCC. Our clinical data indicated that the levels of phosphorylation MEK1/2 and ERK1/2 were increased in HCC comparing with adjacent non-tumorous tissues. It showed the linear correlation between Syncytin-1 expression and upregulated MEK1/2 and ERK1/2 phosphorylation levels in HCC. Furthermore, Syncytin-1 activated MEK/ERK pathway in HCC cells. In-depth research showed that the inflammation-activated MEK/ERK pathway was essential in Syncytin-1 promoted hepatocarcinogenesis. Syncytin-1 suppressed doxorubicin-induced apoptosis via MEK/ERK cascade. In conclusion, Syncytin-1 promoted HCC progression and doxorubicin resistance via the inflammation-activated MEK/ERK pathway. Our findings revealed that Syncytin-1 was a potential prognostic biomarker and therapeutic target for HCC.

Cell Death Discovery (2021)7:177; <https://doi.org/10.1038/s41420-021-00562-5>

INTRODUCTION

Human endogenous retrovirus (HERVs), which originate from exogenous retroviral infections of germ cells millions of years ago, are transmitted to the next generation in a Mendelian manner along with the human genome [1]. The HERVs elements comprise up to around 8% of the human genome [2, 3]. Only a small proportion of the elements encode proteins participating in various biological processes [4]. HERVs have been identified at least 55 families which are categorized into three main classes: Class I, Class II, and Class III [5]. HERV W family belonged to Class I, as a putative causative agent for multiple sclerosis (MS), is one of the most important members of the HERV family [6–8].

Syncytin-1, also known as ERVWE1, is a functional envelope glycoprotein encoded by a single HERV-W env locus that harbors a complete open-reading frame [9]. Syncytin-1 exerts critical functions in the placental trophoblastic formation and maternal immunosuppressive [10, 11]. Abnormal expression of Syncytin-1 participates in inflammation abnormalities of schizophrenia and MS [5, 12].

Recent studies have shown that overexpression of Syncytin-1 is implicated with several types of cancers, including endometrial cancer, breast cancer, leukemia, and urothelial cell carcinoma [13–16]. To the best of our knowledge, there is still no report underlying the role of Syncytin-1 in human hepatocellular carcinoma (HCC).

HCC is the fifth most common cancer and the second cause of cancer-related death worldwide, with more than 840,000 new cases in 2018 [17]. The 5-year survival rate of patients with HCC is 18%, which reflects that most patients failed to be diagnosed at an early stage [18]. Chronic hepatitis B or C virus (HBV, HCV) infections are the major causes leading to HCC [19, 20]. Our previous work has reported that HBV X protein (HBx) induced the overexpression of Syncytin-1 in HepG2 cell line via activating inflammation pathway [21], suggesting that Syncytin-1 might role as a cofactor in HCC pathogenesis. Several inflammation-activated pathways, including mitogen-activated protein kinase (MEK)/extracellular signal-regulated protein kinase (ERK) pathway, are induced in the development of HCC [22, 23]. Combined with

¹State Key Laboratory of Virology and Hubei Province Key Laboratory of Allergy & Immunology, Department of Medical Microbiology, School of Medicine, Wuhan University, 430071 Wuhan, P. R. China. ²Wuxi School of Medicine, Jiangnan University, 214000 Wuxi, P. R. China. ³Department of Biochemistry and Collaborative Innovation Center, Jining Medical University, 272067 Jining, P. R. China. ⁴Department of Infectious Diseases, Renmin Hospital, Wuhan University, 430071 Wuhan, P. R. China. ⁵These authors contributed equally: Yan Zhou, Lijuan Liu. ✉email: fanzhu@whu.edu.cn

Edited by: Inna Lavrik.

Received: 16 March 2021 Revised: 6 May 2021 Accepted: 13 June 2021

Published online: 08 July 2021

Syncytin-1 are a potential oncogene in various metastasis tumors and its capacity to induce inflammation, it will be interesting to investigate the expression pattern of Syncytin-1 in HCC, as well as the relationship between Syncytin-1 and MEK/ERK signal in HCC.

In the present study, bioinformatics analysis showed that Syncytin-1 was highly expressed in HCC tissues compared to the corresponding non-cancerous liver tissues. Analysis *in silico* also pointed out that MEK/ERK pathway was involved in HCC. Our clinical data indicated similar results. Furthermore, overexpression of Syncytin-1 predicted higher tumor stages in HCC. Syncytin-1 was an independent risk factor to predict vascular invasion and poor prognosis in HCC patients. In-depth analysis of clinical data indicated that the levels of phosphorylation MEK1/2 and ERK1/2 showed a linear regression with the expression of Syncytin-1. *In vitro* and *in vivo* assay investigated that Syncytin-1 enhanced cell proliferation, metastasis, and tumorigenicity in HCC. Syncytin-1 was also involved in doxorubicin-resistance in HCC cells. The further study discovered that Syncytin-1 promoted hepatocarcinogenesis and drug resistance via MEK/ERK pathway. In conclusion, these results might provide novel insights into the mechanism underlying the development of HCC, as well as put forward potential therapeutic strategies of HCC.

RESULTS

Syncytin-1 is overexpressed in HCC tissues

To determine the expression level of Syncytin-1 in HCC, bioinformatics analysis using Gene Expression Omnibus (GEO) data (GSE6764) was performed [24]. The result indicated that the expression of Syncytin-1 was significantly higher in HCC tissues than that in normal liver tissues (Fig. 1a). We also collected and determined HCC samples and their corresponding NTs to confirm the bioinformatics results. Quantitative real-time PCR indicated that the mRNA level of Syncytin-1 was ~1.8-fold higher in HCC compared to adjacent tissues ($p < 0.05$, Fig. 1b). Increased mRNA level of Syncytin-1 was observed in 28 of 33 specimens (84.85%) and 7 out of 33 adjacent tissues (21.21%) ($p < 0.001$, Supplementary Table S1). The protein level of Syncytin-1 was about 1.4-fold higher in HCC compared to adjacent tissues ($p < 0.05$, Fig. 1c). Overexpression of Syncytin-1 was observed in 27 of 33 (81.82%) of HCC samples, but only in 8 of 33 (24.24%) of adjacent tissues by western blotting ($p < 0.001$, Supplementary Table S2). Data of immunohistochemistry (IHC) also showed that 84 out of 103 (81.55%) HCC specimens were positively stained, whereas only 13 out of 53 (24.53%) adjacent tissues were positive for Syncytin-1 ($p < 0.001$; Fig. 1d, Supplementary Table S3).

The expression level of Syncytin-1 was also determined in three HCC cell lines by quantitative real-time PCR and western blotting. As shown in Fig. 1e and f, Syncytin-1 was found to be expressed in all the HCC cell lines. Its expression level was higher in HCLM3, which possessed a higher metastatic ability. Taken together, these data indicated that the expression of Syncytin-1 was increased in HCC.

High expression of Syncytin-1 correlates with higher stages of HCC and predicts poor prognosis in HCC patients

To further investigate the role of Syncytin-1 in the progression of HCC, the IHC data were reanalyzed in four stages of HCC tissues. Among the 87 HCC tissues at stages II–IV, 78 (89.66%) showed positive staining of Syncytin-1, whereas only 6 of 16 (37.50%) HCC tissues at stage I were Syncytin-1 positive ($p < 0.001$; Fig. 2a, Table 1). Therefore, the expression of Syncytin-1 was positively correlated with higher stages of HCC. Since the late-stage HCC presented greater invasive and metastatic potential [25], this result suggested that Syncytin-1 might promote the malignant progression of HCC.

We further determined the relationship between Syncytin-1 expression and the other clinicopathologic features using univariate and multivariable Cox regression analysis. Our results

showed that the level of Syncytin-1 in HCC was positively correlated with vascular invasion ($p = 0.004$, Fig. 2b, Table 1) and metastasis ($p < 0.001$, Fig. 2c, Table 1). Since the risk of microvascular invasion and metastasis in HCC increases accompanying larger tumor size [26], we also analyzed the overexpression of Syncytin-1 in HCC with different tumor sizes. The overexpression of Syncytin-1 was significantly related to larger tumor size (>5 cm, $p < 0.001$, Fig. 2d, Table 1). Serum α -fetoprotein (AFP) levels are also a prognostic indicator [27, 28], which may affect prediction, diagnosis, and postoperative prognosis. Our results showed that overexpression of Syncytin-1 occurred more commonly in patients with higher serum AFP levels (>20 $\mu\text{g/L}$, $p = 0.007$) (Fig. 2e, Table 1). The Syncytin-1 expression did not correlate with gender and age using multivariable Cox regression analysis.

Survival analysis of our clinical samples showed that overexpression of Syncytin-1 was positively correlated with poor overall survival (OS, $p = 0.015$, Fig. 2f) and poor disease-free survival (DFS, $p = 0.031$, Fig. 2g). Further study revealed that HCC with high Syncytin-1 expression level had lower median overall survival than HCC without the Syncytin-1 overexpression, regardless of the absence or presence of high serum α -fetoprotein (AFP, Fig. 2h, i). Taken together, it suggested that HCC with a high expression level of Syncytin-1 was prone to have a poor clinical outcome.

The level of Syncytin-1 is significantly associated with HBsAg-positive HCC patients

The molecular mechanisms underlying HBV-induced tumorigenesis remain debated. Our previous research manifested that HBx could induce overexpression of Syncytin-1 through NF- κ B signal in HepG2 cells [14], suggesting Syncytin-1 may serve as a potential cofactor in HBV-related HCC. However, the relationship between Syncytin-1 expression and HBV-induced HCC still needs further investigation. As a result, we analyzed the ratio of Syncytin-1 overexpression in HCC patients with or without serum HBsAg positivity. Interestingly, 81 out of 90 (90.00%) HBsAg-positive HCC patients showed a high protein level of Syncytin-1, while Syncytin-1 overexpression was found only in 3 of 13 (23.08%) HBsAg-negative HCCs (Fig. 2j, Table 1). The ratio of Syncytin-1 overexpression in HCC patients with serum HBsAg positivity was ~3.90 times compared to that of HBsAg-negative HCCs.

In turn, we also evaluated the ratio of serum HBsAg positivity in HCC patients with or without Syncytin-1 overexpression. 81 out of 84 (96.43%) Syncytin-1-positive HCC patients displayed HBsAg positivity in serum, whereas serum HBsAg positivity was found only 9 of 19 (47.37%) in Syncytin-1-negative HCCs (Fig. 2k). Results from the study indicated that the incidence that HCC patients have Syncytin-1 and HBsAg simultaneously expression or not was up to ~88.35% (91/103) (Fig. 2k, Table 1), higher than co-expression incidence that Syncytin-1 with any other clinicopathological parameters. These results suggested a marked consistency between Syncytin-1 expression and HBsAg level.

The multivariate Cox regression test also manifested that HBsAg was positively correlated with Syncytin-1 expression (odds ratio = 12.065, $p < 0.001$, Table 1) in HCC. Spearman rank correlation analysis confirmed that there was a significant positive correlation between the expression of Syncytin-1 and serum HBsAg positivity ($r = 0.573$, $p < 0.001$, Table 2). From the above findings, the enhanced expression of Syncytin-1 might contribute to the progression of HBV-induced HCC.

Syncytin-1 promotes HCC tumorigenicity

To determine the role of Syncytin-1 in HCC tumorigenicity, a series of experiments to detect cell proliferation, cell cycle progression, cell migration, and invasion, and cell malignant transformation were performed. HCC cell lines and NIH3T3, one of the most frequently used cell lines to explore the potential

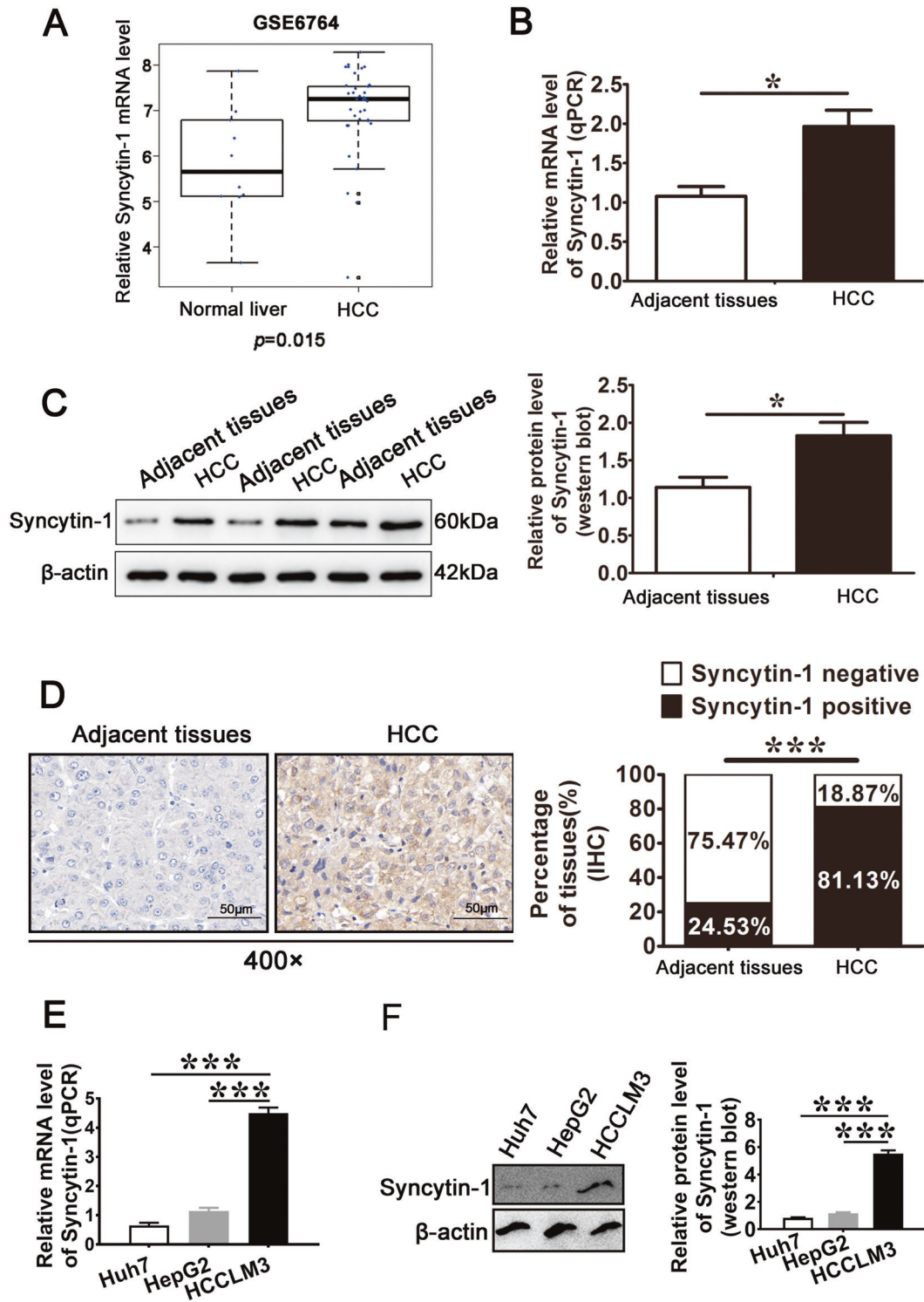


Fig. 1 Synctin-1 is highly expressed in HCC tissues and cell lines. **a** Data from GSE6764 was used to analyze the mRNA level of Synctin-1 in HCC and normal liver. **b** The mRNA level of Synctin-1 was determined by quantitative real-time PCR (qPCR) in HCC and adjacent tissues. **c** Synctin-1 protein levels in 33 pairs of HCC and adjacent tissues were assessed using western blotting. **d** 53 paired of formalin-fixed HCC specimens and 50 formalin-fixed HCC without adjacent tissues (totally 103) were obtained to detect Synctin-1 expression by IHC. Representative images are shown (magnification, $\times 400$). **e** and **f** Synctin-1 mRNA and protein levels in several HCC cell lines were investigated using qPCR (**e**) and western blotting (**f**), respectively. Each bar represents results from three independent experiments. $*p < 0.05$, $***p < 0.001$.

role of an oncogene on cell proliferation and migration in HCC [29, 30], were used. As shown in Fig. 3a, there was a time-dependent increase of cell viability in Synctin-1-transfected NIH3T3 cells using a real-time cell analysis (RTCA) assay.

Knockdown of Synctin-1 expression in HCCLM3 cells by transfecting with pSilencer-shSynctin-1 confirmed the above result (Supplementary Fig. S1a). Correspondingly, the results of cell cycle analysis also verified that Synctin-1 increased the cell

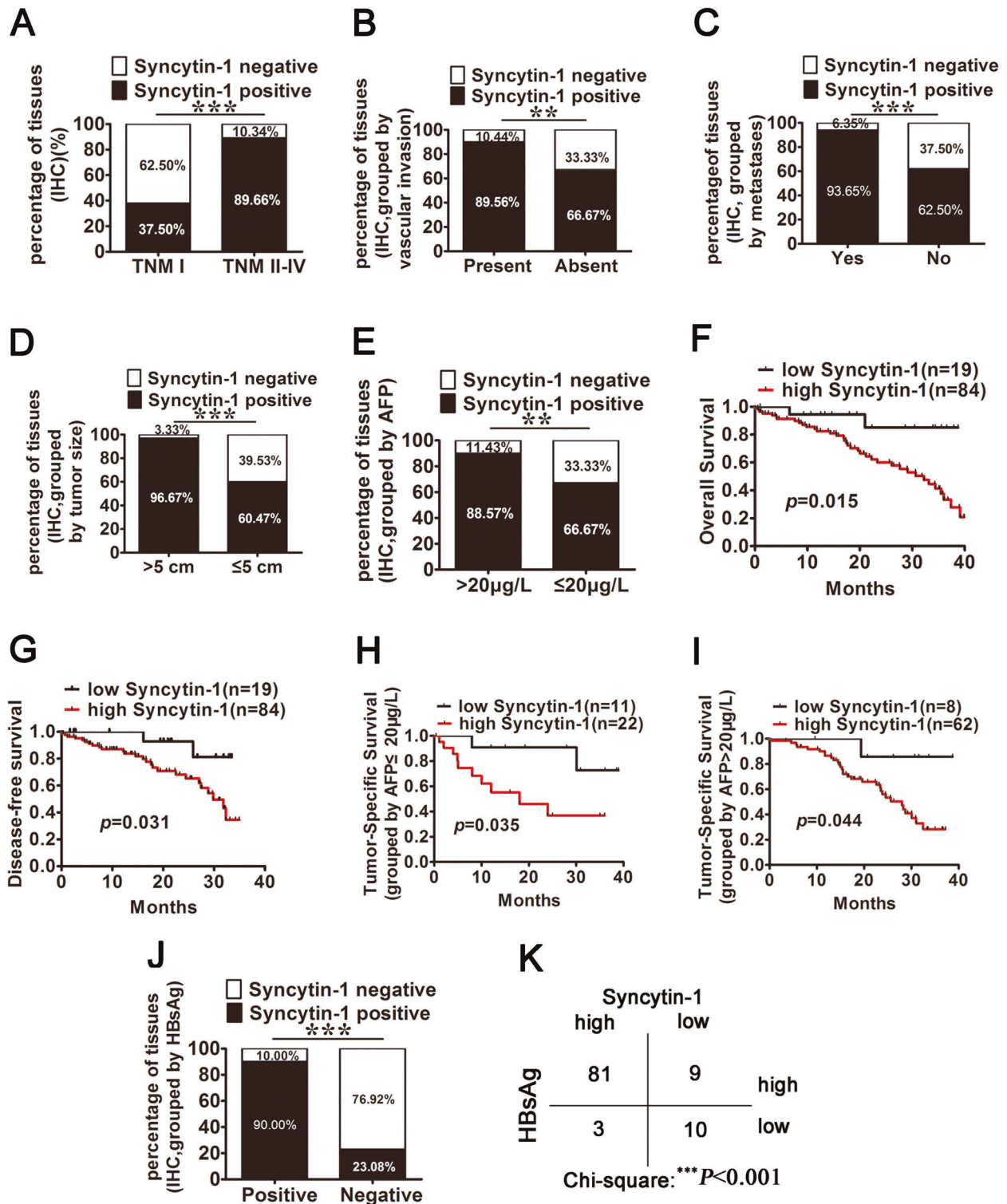


Fig. 2 High expression of Syncytin-1 protein predicts advanced HCC and poor prognosis. The IHC data of Syncytin-1 expression were reanalyzed. **a** The expression of Syncytin-1 was analyzed in four stages of HCC tissues. **b–e** The positivity rate of Syncytin-1 expression in HCC with vascular invasion (**b**), metastases (**c**), different tumor sizes (**d**), and serum level of AFP (**e**) were analyzed. **f–i** Syncytin-1 overexpression was positively correlated with poor overall survival (**f**) and poor disease-free survival (**g**). HCC with high Syncytin-1 expression had a lower median overall survival than HCC without the Syncytin-1 overexpression, regardless of the absence (**h**) or presence (**i**) of high serum AFP. **j** and **k** The overexpression of Syncytin-1 was positive in correlation with serum HBsAg positivity. * $p < 0.05$, ** $p < 0.01$, *** $p < 0.001$.

numbers of S and G2/M stages in both NIH3T3 and HCCLM3 cells ($p < 0.01$, Fig. 3b, Supplementary Fig. S1b). These results suggested that Syncytin-1 could promote proliferation and cell cycle progression in HCC cells.

The metastatic potential of Syncytin-1 was determined by wound healing assay and transwell. The results of the wound healing assay demonstrated that Syncytin-1 improved the mobility of NIH3T3 cells compared to control ($p < 0.01$, Fig. 3c).

Table 1. Univariate and multivariate analysis Syncytin-1 overexpression and various risk factors in 103 HCC patients.

Characteristic	Total N = 103	Univariate analysis		Multivariate analysis				
		Syncytin-1 expression (-)	Syncytin-1 expression (+)	χ^2	p	OR	95% CI	p
Gender				0.009	0.926			NA
Male	66	12(18.18)	54(81.82)					
Female	37	7(18.92)	30(81.08)					
Age (years)				5.213	0.022*	2.286	0.652–8.623	0.153
≤59	60	16(26.67)	44(73.33)					
>59	43	3(6.98)	40(93.02)					
TNM				24.794	<0.001***	10.357 ^a	3.081–48.623	<0.001***
I	16	10(62.50)	6(37.50)					
II	33	4(12.12)	29(87.88)					
III	36	4(11.11)	32(88.89)					
IV	18	1(5.56)	17(94.44)					
Metastases				13.779	<0.001***	5.382	2.208–16.125	<0.001***
Yes	63	4(6.35)	59(93.65)					
No	40	15(37.50)	25(62.50)					
Tumor size (cm)				19.481	<0.001***	8.135	2.574–25.672	<0.001***
≤5	43	17(39.53)	26(60.47)					
>5	60	2(3.33)	58(96.67)					
Microvascular invasion				8.153	0.004**	4.017	1.264–10.683	0.005**
Present	67	7(11.67)	60(89.55)					
Absent	36	12(33.33)	24(66.67)					
HBsAg				29.515	<0.001***	12.065	3.818–82.067	<0.001***
Positive	90	9(10.00)	81(90.00)					
Negative	13	10(76.92)	3(23.08)					
AFP				7.153	0.007**	3.862	1.167–9.853	0.007**
>20 µg/L	70	8(11.43)	62(88.57)					
≤20 µg/L	33	11(33.33)	22(66.67)					

NA not adopted.

* $p < 0.05$, ** $p < 0.01$, *** $p < 0.001$.^aThe OR represents TNM stages II–IV compared to stage I.**Table 2.** Spearman rank correlation analysis of the correlation between Syncytin-1 overexpression and various risk factors in 103 HCC patients.

Characteristic	Syncytin-1 positive	
	r	p
HBsAg positive	0.573	<0.001***
AFP > 20 µg/L	0.264	<0.01**
Tumor size > 5 cm	0.460	<0.001***
TNM II–IV	0.487	<0.001***
Microvascular invasion	0.281	<0.01**
Metastases	0.391	<0.001***

** $p < 0.01$, *** $p < 0.001$.

Conversely, knockdown of Syncytin-1 by pSilencer-shSyncytin-1 transfection inhibited the wound closure of HCCLM3 cells ($p < 0.01$, Supplementary Fig. S1c). The transwell migration assay and invasion assay with matrigel ($p < 0.001$, Fig. 3d, Supplementary Fig. S1d) confirmed the positive effect of Syncytin-1 on cell migration and invasion, respectively. The results above

demonstrated that Syncytin-1 might play a vital role in tumor metastasis.

The function of Syncytin-1 on tumorigenic ability in HCC cells was also investigated. Foci formation assay revealed that NIH3T3-Syncytin-1 cells formed colonies ~5-fold higher than the control ($p < 0.001$, Fig. 3e). After knocking down Syncytin-1 in HCCLM3, the colony-forming ability was almost 75% decreased compared to the control ($p < 0.001$, Supplementary Fig. S1e). Furthermore, tumor xenograft assay showed that Syncytin-1 overexpression in NIH3T3 cells could induce tumor formation at the flank of nude mice, whereas down-regulation of Syncytin-1 expression in HCCLM3 cells effectively inhibited tumor formation ($p < 0.001$, Fig. 3f, Supplementary Fig. S1f, Supplementary Tables S4, 5). These results implicated that Syncytin-1 had oncogenic potential.

The above results indicated that Syncytin-1 could promote the development and progression of HCC.

Syncytin-1 activates the MEK/ERK signal pathway in HCC

Recent studies revealed that the inflammation-activated MEK/ERK pathway was involved in the development of several types of cancers [22, 31, 32]. Bioinformatics analyses using GSE41804 [33] suggested that the genes correlated with HCC were involved in the MEK/ERK pathway, cell cycle, and other pathways in cancer

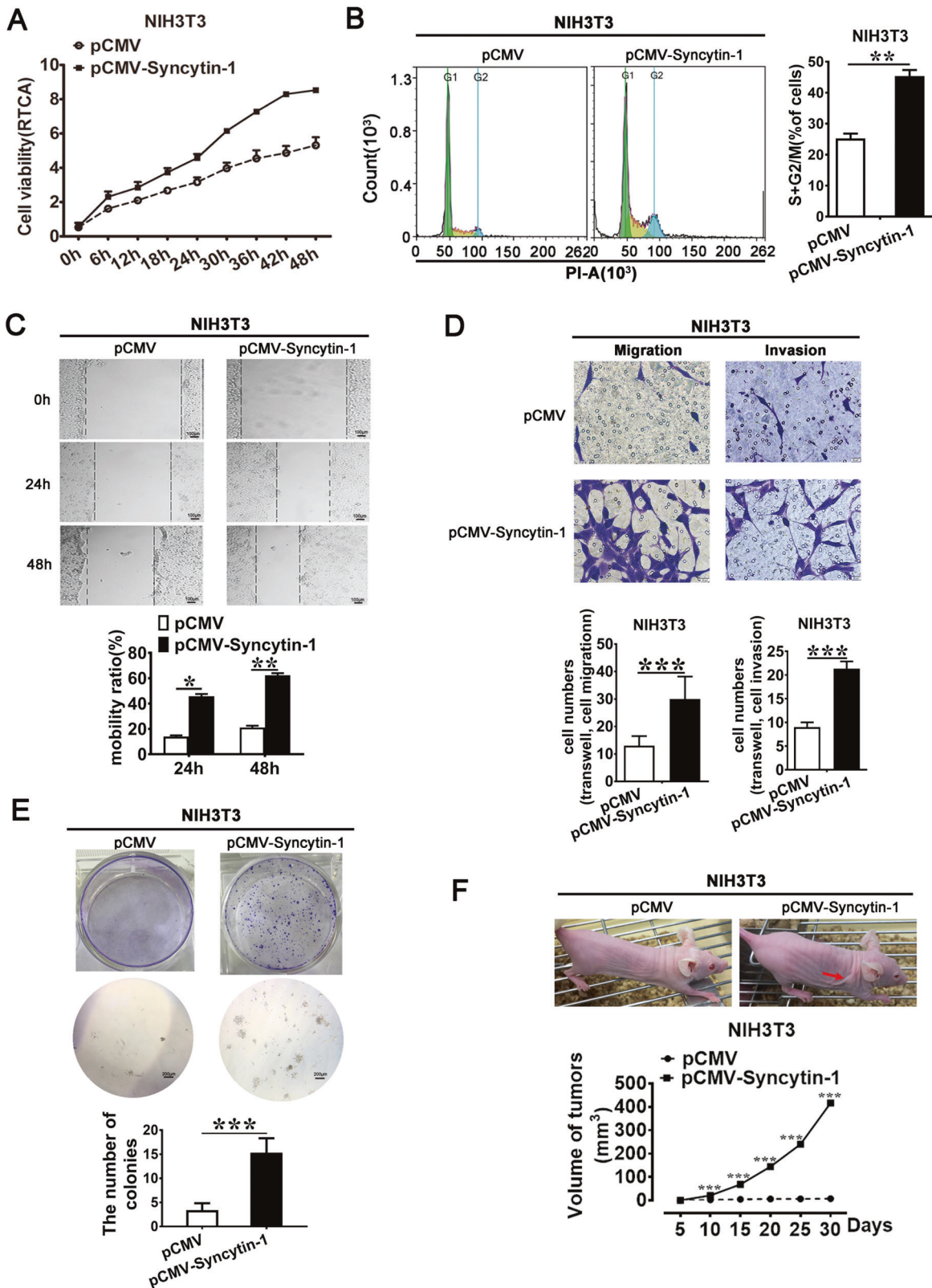


Fig. 3 Syncytin-1 promotes cell marinization in NIH3T3 cells. a The effect of Syncytin-1 on cell proliferation was examined by RATC assay. **b** Variation of the cell cycles in Syncytin-1 overexpressed NIH3T3 cells was determined by flow cytometry. **c** The effect of Syncytin-1 on cell migration ability was assessed using the wound healing assay. **d** The effects of Syncytin-1 on cell migration and invasion were detected. **e** Foci formation assay was used to reveal the role of Syncytin-1 on cell transformation in NIH3T3. **f** Tumor xenograft assay. Arrows indicate the formation of xenograft tumors in nude mice. The graph shows the mean \pm SEM of tumor volume induced by Syncytin-1-transfected NIH3T3 cells. All graphs represent at least three independent experiments. *** $p < 0.001$.

(Fig. 4a, Supplementary Fig. S2a, b, and Supplementary Tables S6, 7). An in-depth analysis showed that the patients with high expression levels of MEK1, ERK2, and its downstream gene cyclin D1 (CCND1) were more likely to be associated with the poor OS (Supplementary Fig. S2c–e). Overexpression of ERK1 and the downstream protein cyclin-dependent kinase4 (CDK4) correlated with vascular invasion (Supplementary Fig. S2, f, g). In silico results indicated that MEK/ERK pathway was implicated in the poor progression of HCC.

To further determine whether MEK/ERK pathway was activated in HCC, we detected the phosphorylation level of MEK1/2 (p-MEK1/2) and ERK1/2 (p-ERK1/2) in paired HCC tissues using IHC. As displayed in Fig. 4b, significantly increased p-MEK1/2 ($p < 0.001$) and p-ERK1/2 ($p < 0.001$) levels were found in HCC specimens. These results suggested that MEK/ERK pathway might be activated in HCC tissues. Since accumulation evidence showed that Syncytin-1 could regulate inflammatory abnormalities [5, 34], it is speculated that Syncytin-1 might aberrantly regulate the inflammation-activated pathway in HCC. Interestingly, our clinical analysis indicated that the positive rate of p-MEK1/2 and p-ERK1/2 were significantly higher in Syncytin-1-positive patients than those in Syncytin-1-negative patients (Fig. 4c). To examine the potential relationship between Syncytin-1 and p-MEK/p-ERK, we analyzed the relationship between the expression levels of Syncytin-1 and p-MEK/p-ERK by Pearson correlation analysis. The results displayed a linear regression between Syncytin-1 and p-MEK1/2 ($r = 0.720$, $p < 0.001$) or p-ERK1/2 in HCC patients ($r = 0.627$, $p < 0.001$, Fig. 4d), suggesting that the expression of Syncytin-1 was positively related to the level of p-MEK/p-ERK.

Studies were then performed to assess the effect of Syncytin-1 on the MEK/ERK signal pathway in HCC cell lines. As shown in Supplementary Fig. S3a, western blot analysis revealed the overexpression of Syncytin-1 after transfected with pCMV-Syncytin-1 plasmids in Huh7 cells. The knockdown of Syncytin-1 in HCCLM3 cells was indicated in Supplementary Fig. S3b. It was shown that Syncytin-1 could increase the expression of p-MEK1/2, p-ERK1/2, and its downstream genes, including CCND1, CDK4, c-myc, c-fos, and c-jun in Huh7 cells, while knockdown of Syncytin-1 resulted in a decrease of the MEK/ERK pathway proteins in the HCCLM3 cell line (Fig. 4e). However, Syncytin-1 did not affect the expression of total MEK1/2 and ERK1/2 (Supplementary Fig. S3a, b). To further confirm whether Syncytin-1 upregulated these downstream proteins through activating the MEK/ERK pathway in HCC cells, JTP-74057, an inhibitor of MEK1/2 activity [35], and GDC-0994, a highly selective ERK1/2 inhibitor [36], were used. After transfection of Syncytin-1 in Huh7 cells, the level of Syncytin-1 was significantly increased (Supplementary Fig. S3c). The results showed that JTP-74057 or GDC-0994 treatment effectively reversed the expression of p-MEK1/2, p-ERK1/2, and their downstream proteins (Fig. 4f), without changing of total MEK1/2 and ERK1/2 expression, in Syncytin-1-transfected Huh7 cells (Supplementary Fig. S3c). In conclusion, our results indicated that Syncytin-1 activated MEK/ERK signal pathway in HCC.

Syncytin-1 enhances HCC tumorigenicity through MEK/ERK pathway

The above results showed that Syncytin-1 could induce malignant properties in HCC, as well as activate the MEK/ERK signal pathway. Combined with the MEK/ERK pathway was positively correlated with HCC progression, we speculated that the MEK/ERK signal might play a critical role in Syncytin-1-induced HCC carcinogenesis and metastasis. To prove this hypothesis, specific MEK inhibitor JTP-74057 and ERK inhibitor GDC-0994 were used. RTCA showed that both inhibitors could induce a time-dependent decrease of cell viability in Huh7-Syncytin-1 cells (Fig. 5a). The proportion of Huh7-Syncytin-1 cells in S and G2/M phases was decreased after treatment with both inhibitors (Fig. 5b). These results indicated that Syncytin-1 promoted HCC cell proliferation through MEK/ERK pathway.

To investigate whether Syncytin-1 induced cell malignancy tumorigenesis in HCC via MEK/ERK pathway, foci formation assay was used. As displayed in Fig. 5c, Syncytin-1 induced colony formation was reversible under the treatment of JTP-74057 or GDC-0994 in Huh7 ($p < 0.001$).

Our results also showed that MEK/ERK inhibitors effectively inhibited Syncytin-1-mediated cell migration by wound healing assay ($p < 0.01$, Fig. 5d) and transwell migration assay ($p < 0.01$, Fig. 5e). Transwell invasion assay revealed that both MEK/ERK inhibitors effectively suppressed cell invasion in Huh7-pCMV-Syncytin cells ($p < 0.01$, Fig. 5e). In conclusion, we demonstrated that Syncytin-1 could enhance tumor malignant transformation and metastasis via the MEK/ERK pathway in HCC.

Syncytin-1 prevents doxorubicin-induced apoptosis via MEK/ERK cascade

Doxorubicin is a chemotherapy medication widely used to treat human cancers and mediate the cellular apoptotic effect [37]. Doxorubicin treatment significantly decreased the cell viability of HCCLM3 by cell counting kit-8 (CCK-8) assay ($p < 0.01$, Fig. 6a). Of interest, the protein level of Syncytin-1 was down-regulated with doxorubicin treatment ($p < 0.05$, Fig. 6b). What's more, the levels of p-MEK, p-ERK, CCND1, and CDK4 were also markedly inhibited by doxorubicin treatment (Fig. 6b), suggesting that doxorubicin treatment could suppress the expression of Syncytin-1 and the activation of the MEK/ERK pathway.

To determine the role of Syncytin-1 on doxorubicin-mediated HCC cell apoptosis, Huh7 cells, which with the lower expression level of Syncytin-1, were transfected with pCMV-Syncytin-1 plasmids followed by treatment with doxorubicin. The CCK-8 assay showed that Syncytin-1 induced a significant time-dependent increase of cell viability compared to control in doxorubicin-treated Huh7 cells ($p < 0.01$, Fig. 6c). Additionally, Syncytin-1 increased the levels of p-MEK ($p < 0.001$), p-ERK ($p < 0.01$), CCND1 ($p < 0.05$), and CDK4 ($p < 0.001$), without changing of total MEK1/2 and ERK1/2 expression, in doxorubicin-treated Huh7 cells (Fig. 6d). These results suggested that Syncytin-1 might inhibit doxorubicin-induced apoptosis via MEK/ERK cascade.

DISCUSSION

HCC is one of the most common malignancies worldwide. Despite therapeutic advances, patients with HCC still have a poor survival rate [38]. The presence of microvascular invasion and extrahepatic metastasis leading to progressive development is one of the major causes for its dismal clinical outcome [39, 40]. To improve the survival rate in HCC patients, it is urgent to investigate the biomarkers for the prognosis of HCC with metastasis. In this study, we found that Syncytin-1 might be an independent biomarker of metastatic invasiveness in HCC.

Syncytin-1 was overexpressed in HCC compared to adjacent tissues (Fig. 1), indicating a strong correlation between HCC and the expression level of Syncytin-1. Tumor-node-metastasis (TNM) stage, tumor size, microvascular invasion, and metastasis are prognostic factors in HCC [41]. Our further bioinformatics and clinical data analysis showed that Syncytin-1 overexpression was related to the TNM stage, vascular invasion, metastasis, tumor size (Fig. 2a–e). Additionally, HCC patients with a higher level of Syncytin-1 were more likely associated with worse clinical outcomes (Fig. 2f, g). Taken together, it suggested that Syncytin-1 might contribute to HCC progression. Serum AFP level is usually used to help diagnose patients with HCC [42, 43]. It was interesting that the overexpression of Syncytin-1 was highly related to poor OS, regardless of with or without high serum AFP levels in HCC (Fig. 2h, i), suggesting that Syncytin-1 might be a novel potential diagnostic biomarker for HCC.

Chronic HBV infection is the leading cause of HCC. However, only a minority of HBV carriers eventually develop HCC,

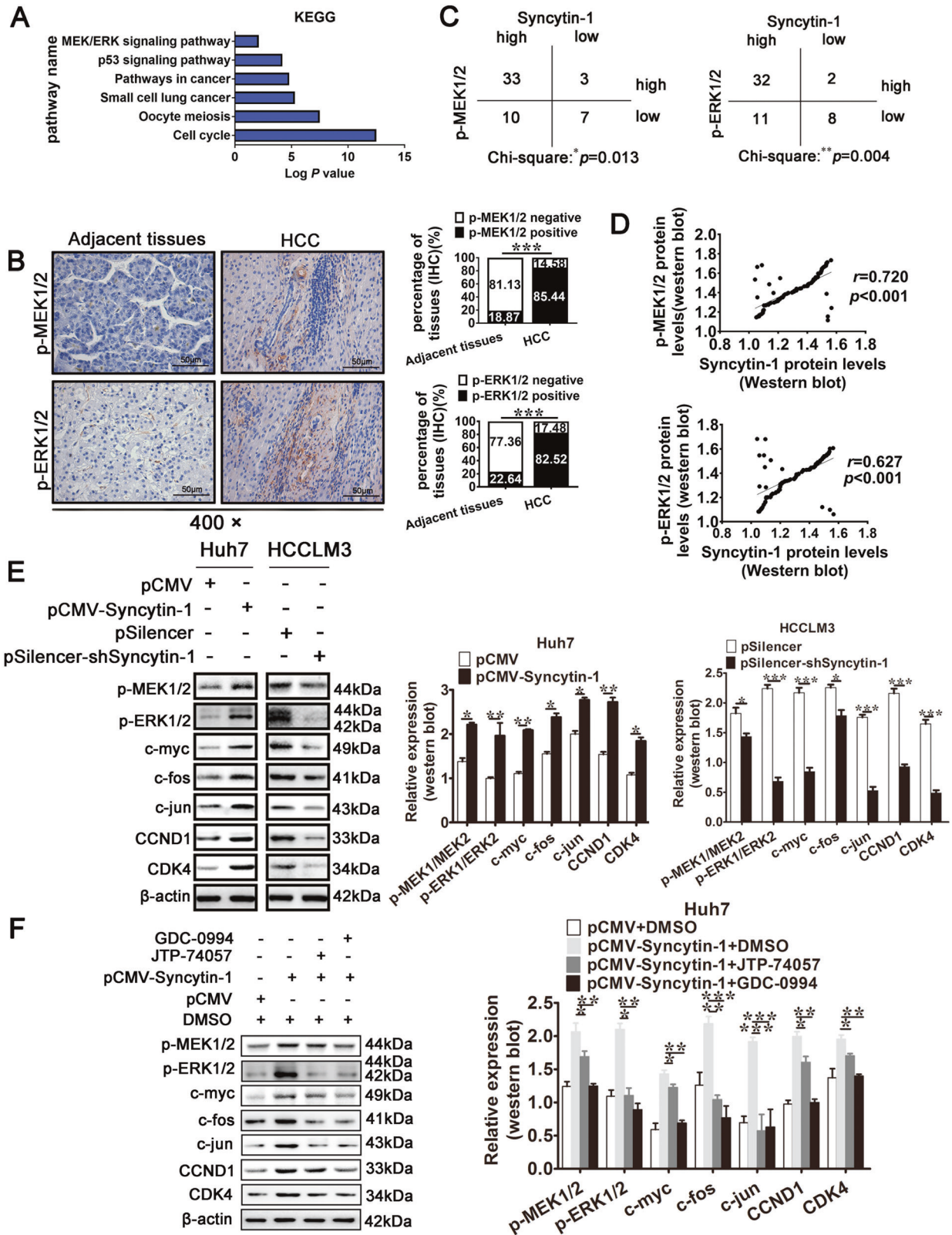


Fig. 4 Syncytin-1 activates MEK/ERK pathway in HCC. **a** The upregulated genes in HCC were analyzed by KEGG analysis. **b** and **c** The expression of p-MEK1/2 and p-ERK1/2 in 53 pairs of formalin-fixed HCC and adjacent tissues were detected using IHC. Representative images are shown (magnification, $\times 400$). **d** The expression of p-MEK1/2 and p-ERK1/2 were determined using western blotting. The correlation between the expression of Syncytin-1 and p-MEK1/2 or p-ERK1/2 level was analyzed using Pearson's correlation test. **e** The levels of p-MEK1/2, p-ERK1/2, and their downstream proteins (c-myc, c-fos, c-jun, CCND1, and CDK4) were examined in HCC cell lines transfected with Syncytin-1 or pSilencer-shSyncytin-1 by western blotting. **f** The levels of p-MEK1/2, p-ERK1/2, and their downstream proteins were detected after using MEK/ERK-specific inhibitors (JTP-74057, or GDC-0994) in Huh7 transfected with Syncytin-1. The bars represent results from at least three independent experiments. * $p < 0.05$, ** $p < 0.01$, *** $p < 0.001$.

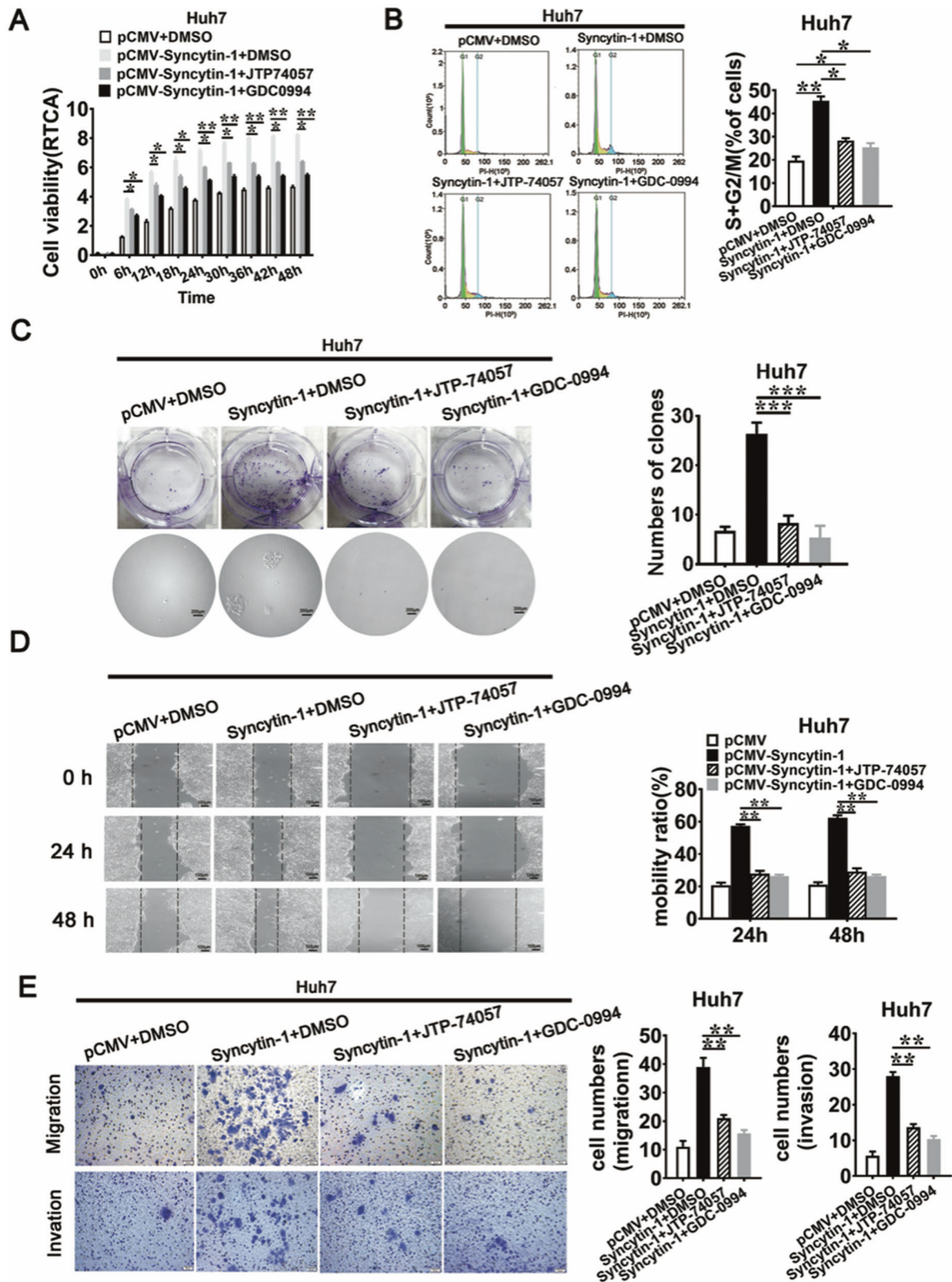
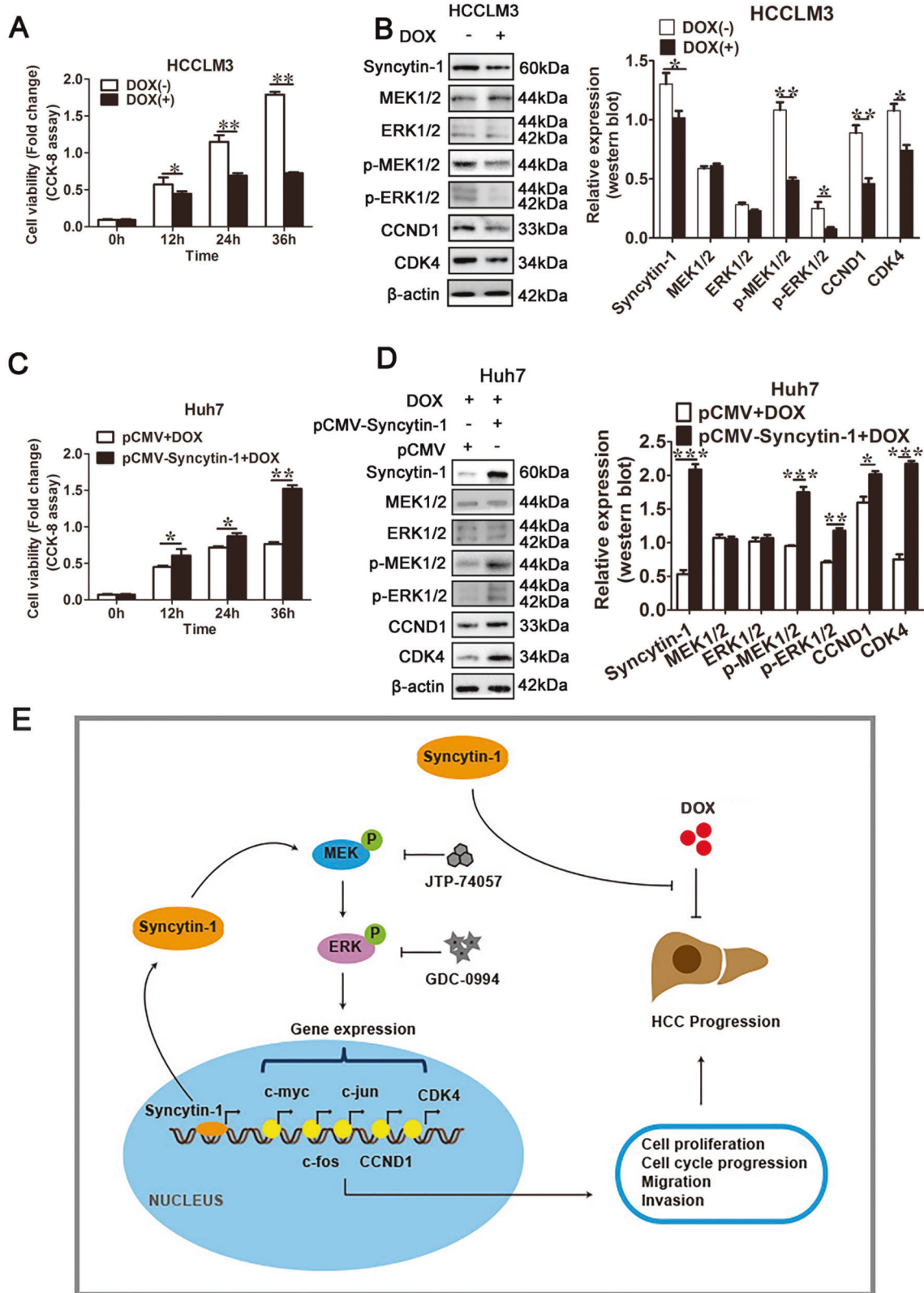


Fig. 5 MEK/ERK signal pathway is necessary for Syncytin-1 induced malignant properties in HCC cells. Huh7 cells transfected with Syncytin-1 were treated with JTP-74057 or GDC-0994, which were specific for MEK/ERK pathway inhibitors. **a** RTCA assay was used to detect the role of Syncytin-1 on cell proliferation when blocking MEK/ERK pathway. **b** Flow cytometry. MEK/ERK signal pathway regulation of Syncytin-1-induced cell cycle progression was demonstrated. **c** The effect of the MEK/ERK pathway on Syncytin-1-induced cell transformation was determined. **d** and **e** The role of the MEK/ERK pathway on Syncytin-1-regulated cell migration or invasion was investigated using wound healing assay (**d**), transwell migration assay, and transwell invasion assay (**e**). All graphs show at least three independent experiments. * $p < 0.05$, ** $p < 0.01$, *** $p < 0.001$.



suggesting the presence of important cofactors in HBV-related HCC [44]. Our previous study has indicated that HBx can act as an oncogene and induce overexpression of Synchronin-1 through NF- κ B in HCC cell lines [21], implying Synchronin-1 might involve in HBV-related HCC. In this study, we showed that Synchronin-1 was

significantly correlated with serum HBsAg positivity (Fig. 2j, k). These results strongly indicated that Synchronin-1 might be a cofactor of HBV in the development of HCC.

Studies have reported that Synchronin-1 promoted proliferation and tumorigenesis in several types of cancers [13–16].

Fig. 6 Syncytin-1 promotes doxorubicin resistance via MEK/ERK pathway in HCC. **a** CCK-8 assay. The effect of doxorubicin on cell viability was determined in HCCLM3 cells. **b** The regulation of doxorubicin on the expression of MEK/ERK pathway protein (MEK1/2, ERK1/2, p-MEK1/2, p-ERK1/2, CCND1, and CDK4) were detected by western blotting. **c** CCK-8 assay was used to investigate the role of Syncytin-1 on doxorubicin-induced cell apoptosis in Huh7 cells. **d** The function of Syncytin-1 overexpression on doxorubicin suppressed MEK/ERK pathway activation was assessed using western blotting. **e** Schema illustrates the mechanism by which Syncytin-1 promotes the development of HCC and doxorubicin resistance through activation of the MEK/ERK pathway. Syncytin-1 induced the activation of the MEK/ERK pathway and upregulation of its downstream proteins (such as c-myc, c-fos, c-jun, CCND1, and CDK4) levels in HCC. These genes participated in the malignant progression of HCC by promoting cell proliferation, migration, and invasion. Syncytin-1 also prevented HCC cells from doxorubicin-induced cell apoptosis. DOX, doxorubicin. * $p < 0.05$, ** $p < 0.01$, *** $p < 0.001$.

To investigate the effect of Syncytin-1 in HCC, several malignant properties of NIH3T3 and HCC cell lines were explored. Our data demonstrated that Syncytin-1 could induce cell proliferation and promote cell cycle progression at the G2/M phase. The wound-healing assay and transwell assay revealed that Syncytin-1 could enhance migration and invasion. Furthermore, foci formation assay and tumor xenograft assay suggested that Syncytin-1 enhanced the tumorigenesis in cell lines (Fig. 3, Supplementary Fig. S1). All these results implicated Syncytin-1 might promote the oncogenic potential of HCC.

Syncytin-1, which served as an immunotoxin, modulates inflammatory cascades [5, 34, 45–47]. Combined with the results that Syncytin-1 had oncogenic potential in HCC (Figs. 1–3), it was highly suggested that Syncytin-1 might promote HCC development through an aberrantly regulated inflammation-activated signal pathway. Bioinformatics prediction and clinical analysis revealed that the MEK/ERK pathway, involved in cancer progression, was activated in HCC (Fig. 4a–b). Further studies indicated that the expression of Syncytin-1 positively correlated with pMEK/pERK level (Fig. 4c, d). We further determined the role of Syncytin-1 on the expression of MEK/ERK pathway proteins. The western blotting analysis showed that the phosphorylation level of MEK1/2, ERK1/2, and the protein level of a series MEK/ERK pathway proteins, including c-myc, c-fos, c-jun, CDK4, and CCND1, were upregulated (Fig. 4e), implying that Syncytin-1 upregulated the expression of MEK/ERK pathway proteins in HCC. Since the downstream proteins had cross-talk with other signal pathways, we further determined whether Syncytin-1 regulated these downstream proteins through MEK/ERK pathway. Two small molecule inhibitors specific to MEK/ERK, JTP-74057, and GDC-0994, were used to block MEK/ERK signal pathway. Our results showed that Syncytin-1-induced upregulation of MEK/ERK and its downstream proteins was suppressed by JTP-74057 or GDC-0994 (Fig. 4f), suggesting that Syncytin-1 regulated the expression of CDK4, CCND1, c-myc, c-fos, and c-jun via the MEK/ERK.

CDK4 and CCND1 are key cell cycle-related genes in controlling cell proliferation [48]. C-myc, c-fos, and c-jun are all proto-oncogenes, involved in the initiation and regulation of oncogenic progression [49–51]. The upregulation of these proteins by the MEK/ERK pathway might contribute to Syncytin-1-induced HCC. Our results have shown that Syncytin-1-induced proliferation and cell cycle progression were reversed after treatment with MEK/ERK pathway inhibitors (Fig. 5a, b). Syncytin-1 also failed to promote migration, invasion, and tumorigenesis in HCC cells when blocking the MEK/ERK pathway (Fig. 5c–e). In summary, this study indicated that Syncytin-1 might enhance carcinogenesis and tumor metastasis in HCC through the MEK/ERK pathway. MEK/ERK pathway can mediate epithelial-to-mesenchymal transition in cancer [52], which is also the potential mechanism that leads to HCC progression.

Doxorubicin is a chemotherapy medication to treat cancer by inducing DNA damage and cell apoptosis [37]. After the treatment of doxorubicin, the viability of HCC cells decreased dramatically, accompanied by significantly down-regulation of Syncytin-1 expression level and the activity of the MEK/ERK pathway (Fig. 6a, b). However, overexpression of Syncytin-1 increased cell viability

and reverted the inhibition of MEK/ERK cascade mediated by doxorubicin compared to control (Fig. 6c, d). These data indicated that Syncytin-1 might induce doxorubicin resistance in HCC cells through the MEK/ERK signal pathway.

In conclusion, our results showed that Syncytin-1 was highly expressed in HCC tissues, and related to advanced HCC. Syncytin-1 was a risk factor, which independent of serum AFP levels, to predict vascular invasion and poor prognosis in HCC patients. Syncytin-1 was also a potential cofactor in HBV-induced HCC. Syncytin-1 might trigger hepatocarcinogenesis and doxorubicin-resistance via the inflammation-activated MEK/ERK pathway (Fig. 6e). These results might provide novel insights into the mechanism underlying the development of HCC, as well as put forward potential therapeutic strategies of HCC.

MATERIALS AND METHODS

Bioinformatics analysis

The Oncomine database (<http://www.oncomine.org/resource/login.html>) was used to predict the expression of Syncytin-1 in HCC. The differentially expressed genes (DEGs) between the HCC and NT were identified using the R programming language's limma package. Studies were performed using the GEO (<http://www.ncbi.nlm.nih.gov/geo>) human HCC microarray dataset with accession numbers GSE6764 [24] and GSE41804 [33] in the GPL570 platform (Affymetrix Human Genome U133 Plus 2.0 Array). With the standard of $|\log_{2}FC| \geq 1$ and p -value < 0.05 , all statistical analyses were performed with R software. The R software was also used to analyze differential gene expression patterns between tumor and normal samples. Gene Ontology (GO) analysis was conducted to demonstrate the functions of the target genes in the biological process, cellular component, and molecular function. Kyoto Encyclopedia of Genes and Genomes (KEGG) pathway analysis was used to excavate remarkable pathways associated with target genes.

Clinical samples

Human HCC tissues and the adjacent tissues ($n = 33$) were collected for quantitative real-time RT-PCR and western blotting analysis. Another 53 paired of formalin-fixed HCC specimens and 50 formalin-fixed HCC without adjacent tissues were obtained for IHC staining. All samples were collected from the patients who underwent surgical resection in Renmin Hospital, Wuhan University, and signed informed consent before their operations. The clinicopathological data of patients were obtained. The 8th edition of the TNM staging system, jointly developed by the American Joint Commission on Cancer (AJCC) and the Union for International Cancer Control (UICC), was used to classify the samples. Sample collections were approved by the Ethics committee of Wuhan University, School of Medicine (Wuhan, China). The study was conducted following the International Ethical Guidelines for Biomedical Research Involving Human Subjects (CIOMS).

Plasmid construction and transfection

Plasmid pCMV-Syncytin-1 was established in our laboratory as described previously [53]. One short hairpin RNA targeting Syncytin-1 (sequence: GGTAACCTCCTCCACACAA) and (control) was cloned into the pSilencer 2.1-U6 neo Vector.

Cells were transiently transfected with indicated plasmid DNA for 48 h using TurboFect Transfection Reagent (Thermo Fisher Scientific, Cleveland, USA) according to the manufacturer's instructions. The corresponding empty vector (pCMV or pSilencer 2.1-U6 neo) was used as a negative control.

Cell culture

HepG2 and NIH3T3 cell lines were purchased from the American type culture collection (ATCC, Manassas, USA). Huh7 cell line was obtained from the Japan Health Science Research Resources Bank (Tokyo, Japan). The HCCLM3 cell line was from the Cell Bank of the China Center for Type Culture Collection (Wuhan, China). The cell lines were cultured at 37 °C with 5% CO₂ in Dulbecco's Modified Eagle Medium (GIBCO, NY, USA) supplemented with 10% fetal bovine serum (GIBCO), 100 units/mL penicillin, and 0.1 mg/mL streptomycin. All experiments were performed with mycoplasma-free cells. The cell lines used in this study have been authenticated by STR profiling.

Pharmacologic treatment

JTP-74057, a highly specific and potent MEK1/2 inhibitor [35], and GDC-0994, a highly selective ERK1/2 inhibitor [36], were used to prevent the activation of the MEK/ERK pathway. Cells were treated with 1 nmol/L JTP-74057 or GDC-0994 in a humidified incubator for 24 h at 37 °C with 5% CO₂.

Doxorubicin is a chemotherapy medication used to treat cancer. Cells were treated with 5 μmol/L doxorubicin for 24 h, followed by the cell counting kit-8 (CCK-8) assay and western blotting.

Quantitative real-time PCR

Total RNA was isolated using Trizol[®] reagents (Invitrogen, Carlsbad, USA). After treating with RNase-free DNase (Promega, WI, USA) to degrade potential DNA contamination, 1 μg RNA was converted into first-stranded DNA by the Reverse Transcriptase ReverTra Ace[™] (TOYOBO, Osaka, Japan). Quantitative real-time PCR was performed in the iCycler System (Bio-Rad, CA, USA) using the SYBR Green PCR master mix (Roch Diagnostics, Mannheim, Germany). The primers used in this study were as follows: Syncytin-1 (Gene ID: 30816) forward: 5'-CCAATGCATCAGG TGGGTAAC-3', Syncytin-1 reverse: 5'-GAGGTACCACAGACAAAAAATATCC T-3'. β-actin was used as an internal control for quantification. The results were given as 2^{-ΔΔCt} values.

Western blotting

HCC tissues and cell lines were lysed using M-PER mammalian protein extraction reagent (Pierce, Thermo Fisher Scientific, Inc.) containing the protease inhibitors following the standard procedures. Protein samples (40 μg) were separated in 4–12% SDS-PAGE gel and transferred onto a nitrocellulose membrane (Amersham Pharmacia Biotech, San Francisco, CA). Western blotting was performed according to the manufacturer's protocols. The following antibodies purchased from Abcam were used in this study: Syncytin-1 (1:2000, ab179693), MEK1/2 (1:5000, ab178876), p-MEK1/2 (S218 + S222) (1:1000, ab194754), c-fos (1:2000, ab208942), c-myc (1:1000, ab32072), c-jun (1:1000, ab31419), CCND1 (1:2000, ab40754), CDK4 (1:1000, ab108357), rabbit IgG (1:2000, ab6721), and β-actin (1:5000, ab227387). ERK1/2 (1:1000, A10613), and p-ERK1 (T202/Y204)/ERK2 (T185/Y187) (1:1000, AP0472) were from ABclonal Technology. β-actin was used as an internal control. The immunoreactive bands were visualized using an ECL reagent (Pierce) according to the manufacturer's recommendation. The bands were quantified by densitometry with ImageJ software (U. S. National Institutes of Health, Bethesda, MD, USA).

IHC

IHC staining was performed according to the standard procedures using the following antibodies: Syncytin-1 (1:200, Abcam, ab179693), p-MEK1/2 (S218 + S222) (1:200, Abcam, ab194754), and p-ERK1 (T202)/ERK2 (T185) (1:200, Abcam, ab201015) were used as primary antibodies. The secondary antibody was Biotinylated goat anti-rabbit IgG (1:1000, CWBIO, cw0156s). Staining intensity was graded as 0 (negative), 1 (weak), 2 (moderate), 3 (strong), and 4 (very strong). Positive samples were scored as 2+, 3+, or 4+. Scores of 0 and 1+ were considered negative.

RTCA

The Real-Time Cell Analyzer (RTCA S16, xCELLigence, ACEA Biosciences, San Diego, CA, USA) was used as described previously to detect the real-time effects of Syncytin-1 on cell proliferation [54]. 5 × 10³ cells were seeded in each well plate with electrodes for 18 h, then treated with different conditions. The sensor analyzer automatically monitored continuously for up to 48 h and expressed as cell index, which represents the cell viability. Cell index values were normalized to the value at the beginning of the treatment.

Flow cytometry

Approximately 1 × 10⁶ cells were harvested and fixed with ice-cold 70% ethanol overnight. The single-cell suspension was prepared and incubated with the staining solution containing 40 μg/mL propidium iodide and 100 μg/mL RNase A for 15 min at room temperature. Then the cell cycle was analyzed by the flow cytometer (FACSAria III, B.D. Bioscience, Breda, The Netherlands) in the Research Center for Medicine and Structural Biology, Wuhan University.

Wound healing assay

The cells in 12-well plates were scratched using a pipette tip. Cell migration into the wound area was monitored and photographed at 0, 24, and 48 h using an inverted phase-contrast microscope (Olympus CH-40, Olympus, Tokyo, Japan). The migration rate was calculated as the proportion of the mean distance between borderlines caused by scratching to the distance, which remained cell-free after migration. Three representative images from each coverslip of the scratched areas under each condition were recorded and averaged.

Transwell assay

For cellular migration assays, cells in serum-free media were seeded into 24-well Transwell[™] chambers (Costar, Cambridge, MA, USA) at 1 × 10⁵ cells/mL. Medium containing 10% FBS was added (500 μL/well) to the lower chambers to serve as the chemoattractant. Incubated at 37 °C for 48 h, the cells that had migrated through the membrane were fixed, stained with crystal violet, and then counted under a microscope (Olympus CH-40).

For cellular invasion assay, transwell with Matrigel (200 μg/mL, B.D. Biosciences, San Jose, CA, USA) was used. The other procedures were the same as above.

Foci formation assay

The cells transfected with indicated plasmids were seeded in six-well plates with 1000 cells per well and incubated at 37 °C. After 2 weeks, the colonies were stained with crystal violet and examined under an Olympus CH-40 microscope (Olympus, Tokyo, Japan). The colony consisted of more than 50 cells were counted.

Tumor xenograft assay

Xenograft tumor assay was used to determine the tumorigenic activity of Syncytin-1 in vivo. Cells were subcutaneously injected into the dorsal flank of BALB/C-nu mice (4–5 weeks old, 15–20 g weight, randomly divided into different groups, with 5 mice per control group and 8 mice per experimental group). Tumor volumes (mm³) were measured every 5 days after injection up to 30 days and calculated using the ellipsoid formula: $4/3 \times \pi \times (L/2 \times W/2 \times H/2)$. All animal care and handling procedures were performed according to the National Institutes of Health's Guide for the Care and Use of Laboratory Animals. Animal experiments were approved by the Animal Ethics Committee of Wuhan University, Wuhan University Center for Animal Experiment/A3 Laboratory.

CCK-8 assay

Approximately 5 × 10³ cells/well were seeded in 96-well plates with 100 μL medium each well. After indicated treatment and incubation, a 10 μL CCK-8 solution was added to each well. The plate was incubated for an additional 2 h before measuring the absorbance at 450 nm wavelength using a microplate reader.

Statistical analysis

The data were from at least three independent randomized trials. All testing was done blind, in duplicate by two technicians. Statistical analyses were conducted using the R-Studio statistical software. Student's *t*-test and one-way ANOVA were used to compare quantitative variables. The Chi-square test was used to analyze qualitative variables. Pearson's correlation test was used to assess the correlation between variables with a normal distribution. Spearman's rank correlation test was used to evaluate the correlation between rank variables. Kaplan–Meier analysis was used for survival analysis. Multivariate analyses were performed using the Cox proportional hazards model. Results were presented as mean ± standard error of the mean (SEM), or mean ± standard deviation (SD). *p* < 0.05 was considered to be significant.

DATA AVAILABILITY

The datasets used and analyzed in this study are available from the corresponding author on reasonable request.

REFERENCES

- de Parseval N, Heidmann T. Human endogenous retroviruses: from infectious elements to human genes. *Cytogenet Genome Res.* 2005;110:318–350.
- Yu HL, Zhao ZK, Zhu F. The role of human endogenous retroviral long terminal repeat sequences in human cancer (Review). *Int J Mol Med.* 2013;32:755–62.
- McPherson JD, Marra M, Hillier L, Waterston RH, Chinwalla A, Wallis J, et al. International Human Genome Mapping Consortium. A physical map of the human genome. *Nature* 2001;409:934–41.
- Mager DL, Stoye JP. Mammalian endogenous retroviruses. *Microbiol Spectr.* 2015;3:0009–2014.
- Wang X, Huang J, Zhu F. Human endogenous retroviral envelope protein syncytin-1 and inflammatory abnormalities in neuropsychological diseases. *Front Psychiatry.* 2018;9:422.
- Mostafa A, Jalilvand S, Shoja Z, Nejati A, Shahmahmoodi S, Sahraian MA, et al. Multiple sclerosis-associated retrovirus, Epstein-Barr virus, and vitamin D status in patients with relapsing remitting multiple sclerosis. *J Med Virol.* 2017;89:1309–13.
- Dolei A. The aliens inside us: HERV-W endogenous retroviruses and multiple sclerosis. *Mult Scler.* 2018;24:42–47.
- Weis S, Llenos IC, Sabuncuyan S, Dulay JR, Isler L, Yolken R, et al. Reduced expression of human endogenous retrovirus (HERV)-W GAG protein in the cingulate gyrus and hippocampus in schizophrenia, bipolar disorder, and depression. *J Neural Transm.* 2007;114:645–55.
- de Parseval N, Lazar V, Casella JF, Benit L, Heidmann T. Survey of human genes of retroviral origin: identification and transcriptome of the genes with coding capacity for complete envelope proteins. *J Virol.* 2003;77:10414–22.
- Tolosa JM, Schjenken JE, Clifton VL, Vargas A, Barbeau B, Lowry P, et al. The endogenous retroviral envelope protein syncytin-1 inhibits LPS/PHA-stimulated cytokine responses in human blood and is sorted into placental exosomes. *Placenta* 2012;33:933–41.
- Mi S, Lee X, Li X, Veldman GM, Finnerty H, Racie L, et al. Syncytin is a captive retroviral envelope protein involved in human placental morphogenesis. *Nature* 2000;403:785–9.
- Groger V, Cynis H. Human endogenous retroviruses and their putative role in the development of autoimmune disorders such as multiple sclerosis. *Front Microbiol.* 2018;9:265.
- Chignola R, Segal M, Molesini B, Baruzzi A, Stella S, Milotti E. Collective radio-resistance of T47D breast carcinoma cells is mediated by a Syncytin-1 homologous protein. *PLoS ONE.* 2019;14:e206713.
- Liu C, Xu J, Wen F, Yang F, Li X, Geng D, et al. Upregulation of syncytin-1 promotes invasion and metastasis by activating epithelial-mesenchymal transition-related pathway in endometrial carcinoma. *Oncotargets Ther.* 2019;12:31–40.
- Sun Y, Zhu H, Song J, Jiang Y, Ouyang H, Dong T, et al. Expression of leukocytic syncytin-1 in B-cell acute lymphoblastic leukemia and acute myeloid leukemia patients. *Clin Lab.* 2017;63:1567–74.
- Yu H, Liu T, Zhao Z, Chen Y, Zeng J, Liu S, et al. Mutations in 3'-long terminal repeat of HERV-W family in chromosome 7 upregulate syncytin-1 expression in urothelial cell carcinoma of the bladder through interacting with c-Myb. *Oncogene* 2014;33:3947–58.
- European Association for the Study of the Liver. EASL Clinical Practice Guidelines: management of hepatocellular carcinoma. *J Hepatol.* 2018;69:182–236.
- Yarchoan M, Agarwal P, Villanueva A, Rao S, Dawson LA, Llovet JM, et al. Recent developments and therapeutic strategies against hepatocellular carcinoma. *Cancer Res.* 2019;79:4326–30.
- Fujiwara N, Friedman SL, Goossens N, Hoshida Y. Risk factors and prevention of hepatocellular carcinoma in the era of precision medicine. *J Hepatol.* 2018;68:526–49.
- Levero M, Zucman-Rossi J. Mechanisms of HBV-induced hepatocellular carcinoma. *J Hepatol.* 2016;64:584–5101.
- Liu C, Liu L, Wang X, Liu Y, Wang M, Zhu FHBV. X Protein induces overexpression of HERV-W env through NF- κ B in HepG2 cells. *Virus Genes.* 2017;53:797–806.
- Ji Y, Wang Z, Chen H, Zhang L, Zhuo F, Yang Q. Serum from chronic hepatitis B patients promotes growth and proliferation via the IGF-1/IGF-1R/MEK/ERK signaling pathway in hepatocellular carcinoma cells. *Cell Physiol Biochem.* 2018;47:39–53.
- Zhang Q, Wei L, Yang H, Yang W, Yang Q, Zhang Z, et al. Bromodomain-containing protein represses the Ras/Raf/MEK/ERK pathway to attenuate human hepatoma cell proliferation during HCV infection. *Cancer Lett.* 2016;371:107–16.
- Wurmbach E, Chen YB, Khitrov G, Zhang W, Roayaie S, Schwartz M, et al. Genome-wide molecular profiles of HCV-induced dysplasia and hepatocellular carcinoma. *Hepatology* 2007;45:938–47.
- Colagrande S, Inghilesi AL, Aburas S, Taliani GG, Nardi C, Marra F. Challenges of advanced hepatocellular carcinoma. *World J Gastroenterol.* 2016;22:7645–59.
- Trevisani F, Cantarini MC, Wands JR, Bernardi M. Recent advances in the natural history of hepatocellular carcinoma. *Carcinogenesis* 2008;29:1299–305.
- Han JH, Kim DG, Na GH, Kim EY, Lee SH, Hong TH, et al. Evaluation of prognostic factors on recurrence after curative resections for hepatocellular carcinoma. *World J Gastroenterol.* 2014;20:17132–40.
- Tandon P, Garcia-Tsao G. Prognostic indicators in hepatocellular carcinoma: a systematic review of 72 studies. *Liver Int.* 2009;29:502–10.
- Lee SA, Kim H, Won YS, Seok SH, Na Y, Shin HB, et al. Male-specific hepatitis B virus large surface protein variant W4P potentiates tumorigenicity and induces gender disparity. *Mol Cancer.* 2015;14:23.
- Lee MJ, Xu DY, Li H, Yu GR, Leem SH, Chu IS, et al. Pro-oncogenic potential of NM23-H2 in hepatocellular carcinoma. *Exp Mol Med.* 2012;44:214–24.
- Yoshitake R, Saeki K, Eto S, Shinada M, Nakano R, Sugiyama H, et al. Aberrant expression of the COX2/PGE2 axis is induced by activation of the RAF/MEK/ERK pathway in BRAFV595E canine urothelial carcinoma. *Sci Rep.* 2020;10:7826.
- Ramaswamy P, Goswami K, Dalavaikodihalli NN, Srinivas D, Prasad C. TNF- α mediated MEK-ERK signaling in invasion with putative network involving NF- κ B and STAT-6: a new perspective in glioma. *Cell Biol Int.* 2019;43:1257–66.
- Hodo Y, Honda M, Tanaka A, Nomura Y, Arai K, Yamashita T, et al. Association of interleukin-28B genotype and hepatocellular carcinoma recurrence in patients with chronic hepatitis C. *Clin Cancer Res.* 2013;19:1827–37.
- Wang X, Liu Z, Wang P, Li S, Zeng J, Tu X, et al. Syncytin-1, an endogenous retroviral protein, triggers the activation of CRP via TLR3 signal cascade in glial cells. *Brain Behav Immun.* 2018;67:324–34.
- Gilmartin AG, Bleam MR, Groy A, Moss KG, Minthorn EA, Kulkarni SG, et al. GSK1120212 (JTP-74057) is an inhibitor of MEK activity and activation with favorable pharmacokinetic properties for sustained in vivo pathway inhibition. *Clin Cancer Res.* 2011;17:989–1000.
- Varga A, Soria JC, Hollebecque A, LoRusso P, Bendell J, Huang SA, et al. A First-in-Human Phase I Study to evaluate the ERK1/2 Inhibitor GDC-0994 in patients with advanced solid tumors. *Clin. Cancer Res.* 2020;26:1229–36.
- Yang F, Teves SS, Kemp CJ, Henikoff S. Doxorubicin, DNA torsion, and chromatin dynamics. *Biochim Biophys Acta.* 2014;1845:84–89.
- Bray F, Ferlay J, Soerjomataram I, Siegel RL, Torre LA, Jemal A. Global cancer statistics 2018: GLOBOCAN estimates of incidence and mortality worldwide for 36 cancers in 185 countries. *CA Cancer J Clin.* 2018;68:394–424.
- Lim KC, Chow PK, Allen JC, Chia GS, Lim M, Cheow PC, et al. Microvascular invasion is a better predictor of tumor recurrence and overall survival following surgical resection for hepatocellular carcinoma compared to the Milan criteria. *Ann Surg.* 2011;254:108–13.
- Uka K, Aikata H, Takaki S, Shirakawa H, Jeong SC, Yamashina K, et al. Clinical features and prognosis of patients with extrahepatic metastases from hepatocellular carcinoma. *World J Gastroenterol.* 2007;13:414–20.
- Selçuk H. Prognostic factors and staging systems in hepatocellular carcinoma. *Exp Clin Transpl.* 2017;15:45–49.
- Huo L, Wei W, Yan Z, Lei Z, Xie Y, Gong R, et al. Short-term and long-term outcomes of liver resection for HCC patients with portal vein tumor thrombus. *Cell Biosci.* 2019;9:23.
- Bai DS, Zhang C, Chen P, Jin SJ, Jiang GQ. The prognostic correlation of AFP level at diagnosis with pathological grade, progression, and survival of patients with hepatocellular carcinoma. *Sci Rep.* 2017;7:12870.
- Yu MC, Yuan JM, Lu SC. Alcohol, cofactors and the genetics of hepatocellular carcinoma. *J Gastroenterol Hepatol.* 2008;23:592–597.
- Wang X, Wu X, Huang J, Li H, Yan Q, Zhu F. Human endogenous retrovirus W family envelope protein (HERV-W env) facilitates the production of TNF- α and IL-10 by inhibiting MyD88s in glial cells. *Arch Virol.* 2021;166:1035–45.
- Tu X, Li S, Zhao L, Xiao R, Wang X, Zhu F. Human leukemia antigen-A*0201-restricted epitopes of human endogenous retrovirus W family envelope (HERV-W env) induce strong cytotoxic T lymphocyte responses. *Virology* 2017;32:280–9.
- Xiao R, Li S, Cao Q, Wang X, Yan Q, Tu X, et al. Human endogenous retrovirus W env increases nitric oxide production and enhances the migration ability of microglia by regulating the expression of inducible nitric oxide synthase. *Virology* 2017;32:216–25.
- Schade AE, Oser MG, Nicholson HE, DeCaprio JA. Cyclin D-CDK4 relieves cooperative repression of proliferation and cell cycle gene expression by DREAM and R.B. *Oncogene* 2019;38:4962–76.
- Ding Y, Hao K, Li Z, Ma R, Zhou Y, Zhou Z, et al. c-Fos separation from Lamin A/C by GDF15 promotes colon cancer invasion and metastasis in inflammatory microenvironment. *J Cell Physiol.* 2020;235:4407–21.
- Lukey MJ, Greene KS, Erickson JW, Wilson KF, Cerione RA. The oncogenic transcription factor c-Jun regulates glutaminase expression and sensitizes cells to glutaminase-targeted therapy. *Nat Commun.* 2016;7:11321.
- Dang CV. MYC on the path to cancer. *Cell.* 2012;149:22–35.

52. Ding C, Luo J, Li L, Li S, Yang L, Pan H, et al. Gab2 facilitates epithelial-to-mesenchymal transition via the MEK/ERK/MMP signaling in colorectal cancer. *J Exp Clin Cancer Res.* 2016;35:5.
53. Huang W, Li S, Hu Y, Yu H, Luo F, Zhang Q, et al. Implication of the env gene of the human endogenous retrovirus W family in the expression of BDNF and DRD3 and development of recent-onset schizophrenia. *Schizophr Bull.* 2011;37:988–1000.
54. Liu Y, Liu L, Zhou Y, Zhou P, Yan Q, Chen X, et al. CKLF1 enhances inflammation-mediated carcinogenesis and prevents doxorubicin-induced apoptosis via IL6/STAT3 signaling in HCC. *Clin Cancer Res.* 2019;25:4141–54.

ACKNOWLEDGEMENTS

We are grateful to the contributors of the human HCC microarray dataset with accession numbers GSE6764 and GSE41804 in the GPL570 platform (Affymetrix Human Genome U133 Plus 2.0 Array) to the Gene Expression Omnibus (GEO) (<http://www.ncbi.nlm.nih.gov/geo>). Many thanks to the Research Center for Medicine and Structural Biology of Wuhan University for providing the flow cytometer (FACS Aria III, B.D. Bioscience) and the Real-Time Cell Analyzer (RTCA S16, xCELLigence). This work was supported by the National Natural Science Foundation of China (81971943 and 81772196), the Chinese foundation for hepatitis prevention and control (TQGB 20170068), the Hubei Provincial Natural Science Foundation of China (2020CFB656), and the Medical Science Advancement Program (Clinical Medicine) of Wuhan University (TFCLC 2018003).

AUTHOR CONTRIBUTIONS

FZ designed the study. YZ, LJJ, YYL, and HLY performed the study and participated in the analysis of the data. PZ and QJY analyzed the data. XBC provided the clinical samples and managed their information. YZ, LJJ, and FZ co-wrote and revised the paper. All authors read and approved the final manuscript.

COMPETING INTERESTS

The authors declare no competing interests.

ETHICS STATEMENT

All human samples were obtained with informed consent. Sample collections were approved by the Ethics committee of Wuhan University, School of Medicine (Wuhan, China). The study was conducted following the International Ethical Guidelines for Biomedical Research Involving Human Subjects (CIOMS).

ADDITIONAL INFORMATION

Supplementary information The online version contains supplementary material available at <https://doi.org/10.1038/s41420-021-00562-5>.

Correspondence and requests for materials should be addressed to F.Z.

Reprints and permission information is available at <http://www.nature.com/reprints>

Publisher's note Springer Nature remains neutral with regard to jurisdictional claims in published maps and institutional affiliations.



Open Access This article is licensed under a Creative Commons Attribution 4.0 International License, which permits use, sharing, adaptation, distribution and reproduction in any medium or format, as long as you give appropriate credit to the original author(s) and the source, provide a link to the Creative Commons license, and indicate if changes were made. The images or other third party material in this article are included in the article's Creative Commons license, unless indicated otherwise in a credit line to the material. If material is not included in the article's Creative Commons license and your intended use is not permitted by statutory regulation or exceeds the permitted use, you will need to obtain permission directly from the copyright holder. To view a copy of this license, visit <http://creativecommons.org/licenses/by/4.0/>.

© The Author(s) 2021, corrected publication 2022